Theory of tetrahedral-site interstitial s- and p-bonded impurities in Si

Otto F. Sankey and John D. Dow

*Department of Physics and Materials Research Laboratory, University of Illinois
at Urbana-Champaign, 1110 West Green Street, Urbana, Illinois 61801*

(Received 2 August 1982)

A theory of the major chemical trends in the deep-energy levels of interstitial defects at the tetrahedral site in semiconductors is developed, based on a simple, empirical tight-binding scheme. The importance of hyperdeep and hyperbonding levels is emphasized. The theory is applied to various charge states of 29 interstitial defects in Si with the use of a self-consistent defect potential. The theory accounts for the electron-nuclear double-resonance data of the deep Al^{2+} wave function and the deep-energy levels of Al^{+}, as well as for what is currently known about the major chemical trends in the deep and shallow levels of several other impurities.

I. INTRODUCTION

The purpose of this paper is to develop a simple theory of the electronic energy levels introduced into or near the fundamental band gap of Si by an s-p—bonded impurity occupying an interstitial site of tetrahedral symmetry. Our major goal is to establish guidelines, based on the valence, atomic properties, and chemistry of the defect, for predicting which interstitial impurities are likely to act as shallow donors, shallow acceptors, deep donors, deep acceptors, or inert centers.

Some such guidelines for the energy levels of defects already exist for *substitutional* impurities; for example, a substitutional defect whose valence differs from that of the host by $+1$ (-1) typically forms a shallow hydrogenic donor (acceptor) level. Although this simple rule for substitutional defects has a number of important exceptions, it acts as a useful rule of thumb for anticipating the character of common dopants. However, no analogous rule exists for interstitial impurities.

Interstitial impurities play an important role in semiconductors. Some, such as Li, Mg, and the transition metals in Si, energetically prefer to occupy the interstitial site and are electrically active. Other impurities are driven, via the Watkins exchange mechanism,[1] from the substitutional site to the interstitial site as a result of radiation damage. Interstitials are also important in atomic migration, since the diffusion constant for an interstitial impurity is typically several orders of magnitude larger than for a substitutional impurity. Furthermore, in the II-VI materials, it is believed that a substitutional group-I acceptor may spontaneously move to an interstitial site,[2] thereby becoming a donor and self-compensating the material.[3]

In the present work, we select the tetrahedral interstitial site in Si as a prototype because of its high symmetry, its fourfold coordination, and the fact that the nearest-neighbor bond length for the interstitial is the same as that of a bulk host atom. We expect the basic mathematical methods and physical ideas developed for this prototypical site to apply to other lower-symmetry interstitial sites as well.

Most of the theoretical work on interstitial impurities has been concerned with the transition-metal impurities[4,5] because of their technological importance in semi-insulating material. It has been known for some time from spin-resonance experiments[6] that these transition-metal impurities occupy tetrahedral sites and produce a number of levels in the band gap associated with different charge states of the impurity.

Much less theoretical work has been devoted to impurities with an outer s-p valence structure. This is partly due to a lack of detailed experimental information concerning their energy levels and site symmetries. Yamaguchi[7] and Weigel et al.[8] have investigated interstitial carbon in diamond. The Li interstitial in Si has been investigated by Singh et al.[9] and the self-interstitial in Si by Singhal[10] and more recently by Kauffer et al.,[11] Weigel,[12] and Scheffler et al.[13] However, all of these calculations, except those of Weigel,[12] consider only one specific impurity, so they provide little insight into the global chemical trends in the defect energy levels. Our approach is to consider a large number of impurities so that the general systematics of the energy levels will be displayed, even if some imprecision results for the

energy levels of individual defects.

We treat the host Hamiltonian H_0 using the empirical tight-binding nearest-neighbor approximation: Thus the host Si bands are determined by the Vogl *et al.* $10N \times 10N \, sp^3 s^*$ model Hamiltonian matrix,[14] where N is the number of unit cells. The interstitial impurity is treated by augmenting the $10N$ host basis orbitals and including in addition one s orbital and three p orbitals centered at the interstitial site. Hence the (uncoupled) Hamiltonian matrix for the host plus interstitial impurity (in the localized basis) is a direct sum $H^0 \oplus H^I$, where H^I is the diagonal 4×4 interstitial Hamiltonian. The coupling W between the host and the interstitial impurity is a $10N \times 4$ sparse matrix. The matrix elements of W vanish except between the interstitial and its 10 closest neighboring atoms. The nonzero matrix elements between neighbors are assumed to depend only on the bond length and on the relative symmetries and orientations of the orbitals involved (viz., there are eight independent nonzero matrix elements: $W_{ss\sigma}$, $W_{sp\sigma}$, $W_{pp\pi}$, and $W_{pp\sigma}$ for nearest and for second-nearest neighbors; each W scales with distance according to the Pandey-Phillips rule[15]). The chemical identity of the interstitial-impurity atom is contained exclusively in its central-cell potential, namely, the four diagonal elements of H^I. These diagonal elements, in the case of a Si self-interstitial, are taken to be equal to the Si-site diagonal elements of H_0. For an interstitial impurity other than neutral Si, additions V_s and V_p are made to the diagonal matrix elements; these are determined in a self-consistent manner using the ideas of Haldane and Anderson.[16] We found this to be necessary since an interstitial atom is not in general neutrally charged within its atomic volume. Moreover, we expect some interstitial impurities, especially those that are highly charged, to exhibit bonding characteristics quite different from the highly covalent sp^3 tetrahedral bonding. Except for this self-consistency requirement (which is less important for substitutional defects) this theory is similar to an earlier model of substitutional deep traps by Hjalmarson *et al.*[17]

The remainder of this paper is organized into three main sections. The theory is given in Sec. II and consists of two parts: (a) the construction of the Green's-function equation for the determination of the bound-state eigenenergies for a given central-cell potential, and (b) the evaluation of the central-cell interstitial atomic potential for a particular impurity using the procedure of Haldane and Anderson. A discussion of the essential qualitative physics governing interstitial deep levels is described in Sec. III, including illustrations of the main features of the wave functions and the dependence of the deep-

energy levels on the interstitial impurity and its local chemistry. In Sec. IV, the results of the present theory for 29 different s-p—bonded tetrahedral-interstitial-site impurities in a number of different charge states are given and compared with available data; most notably the theory for Al^{2+} is compared with the wave function extracted from electron-spin-resonance (ESR) and electron-nuclear double-resonance (ENDOR) experiments. Finally in Sec. V we summarize our findings and discuss our conclusions.

II. THEORY

A. The eigenvalue equation

We now construct the eigenvalue equation for the defect energy levels of an interstitial impurity in Si with a *given* 4×4 central-cell potential matrix. (The question of how the central-cell potential for a specific impurity is determined will be addressed in the following section.) The basis set of the Si host crystal in the tight-binding approximation is augmented by introducing localized orbitals centered on the interstitial site. This is necessary because expansion of the interstitial wave function in terms of the wave functions of the nearby host Si atoms is doomed to slow convergence.[18] Thus the model Hamiltonian in the localized orbital basis takes the schematic block form

$$H = \begin{bmatrix} H^0 & W \\ W^\dagger & H^I \end{bmatrix}, \tag{1}$$

where H^0 is the perfect-crystal host Si Hamiltonian of Vogl *et al.*,[14] H^I is the interstitial Hamiltonian in an appropriate basis (we shall use an sp^3 basis at the interstitial site), and W denotes the coupling matrix elements between the interstitial atom and the host. The localized orbitals we use for all of the matrix elements in this section will be assumed to have the same spin component, say spin up ($\uparrow$). All matrix elements between spin orbitals with opposite spin components vanish since we have neglected spin-orbit interactions. The interstitial Hamiltonian H_I is a 4×4 diagonal matrix with elements $\epsilon_s(I)$, $\epsilon_p(I)$, $\epsilon_p(I)$, and $\epsilon_p(I)$ equal to the interstitial s, p_x, p_y, and p_z orbital energies "in the solid," respectively. For the case of the neutral Si self-interstitial these orbital energies in the solid are taken to be the on-site matrix elements in the Vogl *et al.* Si tight-binding Hamiltonian, because the coordination numbers and the bond lengths are the same for the neutral interstitial Si and for host Si: A neutral *interstitial* Si atom has the same on-site matrix elements $\epsilon(I)$ as a *host* Si atom. For interstitial impurities other than

neutral Si, the matrix elements $\epsilon(I)$ will be discussed below.

The geometric configuration of the tetrahedral-site interstitial is shown in Fig. 1. There are four nearest neighbors (1, 2, 3, and 4) at a distance d (2.35 Å in Si) and six second-nearest neighbors ($1'$, $2'$, $3'$, $4'$, $5'$, and $6'$) at a slightly greater distance $1.15d$. In a crude approximation the interstitial may be thought of as tenfold coordinated. It is interesting to compare the tetrahedral-interstitial site with a substitutional site which also has four nearest neighbors at a distance d but twelve second-neighbor atoms at the much larger distance $1.63d$, and hence is fourfold coordinated. Even though the nearest-neighbor environments are nominally identical, it is important to note that the interstitial's four neighbors each have four completely saturated tetrahedral bonds prior to the introduction of the interstitial, and so, while the interstitial atom has four neighbors to which it bonds, each of its neighbors must bond to five atoms: the four original neighbors of the host plus the interstitial. As a result, the newly formed levels generated by the presence of the interstitial impurity tend to be associated with either (i) the impurity's atomic energy levels (the host couples only weakly to the defect and acts like a dielectric cage) or (ii) modifications of the chemical bonding of the neighboring host atoms.

The coupling of the interstitial atom to its neigh-
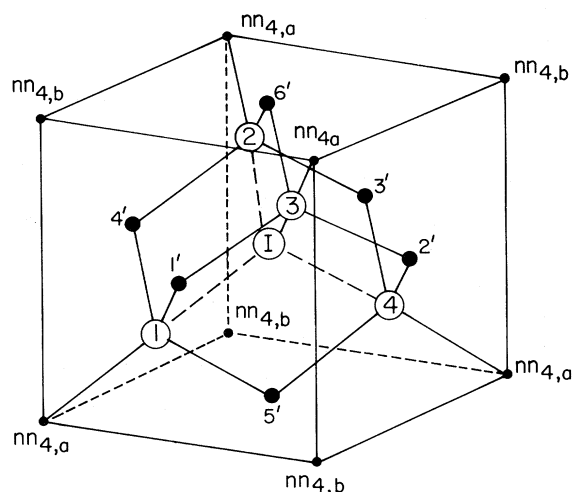
FIG. 1. Geometrical surroundings of an interstitial impurity I at the tetrahedral-interstitial site. The nearest neighbors are denoted 1, 2, 3, and 4; the second-nearest neighbors are labeled $1'$, $2'$, $3'$, $4'$, $5'$, and $6'$; and the two inequivalent shells of equidistant fourth-nearest neighbors are labeled $nn_{4,a}$ (for atoms bonded to nearest neighbors) and $nn_{4,b}$. The third-nearest neighbors lie outside the cube of the figure. Note that the second neighbors are almost as close to the interstitial as the first neighbors, and therefore can bond directly to it.

bors is described by the transfer matrix W. We assume that all transfer matrix elements vanish except those between the interstitial atom and its four nearest neighbors (atoms 1 through 4 in Fig. 1) and its six second neighbors (atoms $1'$ through $6'$). The nearest-neighbor parameters are taken to be those of the Vogl et al.[14] tight-binding model, since these four atoms form an environment about the interstitial that is locally identical to that about a substitutional atom. The second shell of neighbors (nn_2) is very nearly as close to the defect as the first shell (nn_1); so we approximate all these second-neighbor interactions by scaling the nearest-neighbor interactions with distance according to the exponential scaling factor of Pandey and Phillips,[15]

$$W_{nn_2} = W_{nn_1} \exp^{-(6.06\delta d/d)} . \tag{2}$$

Here δd is the difference between the first- and the second-neighbor distances. The parameters used in the model are listed in Table I. The above scaling rule has not been justified in any rigorous sense, but by comparing it with other scaling schemes [i.e., as overlap integrals of atomic wave functions[19] or as d^{-2} (Ref. 20)] we find the most important feature to be that the second-shell interactions be included in some reasonable approximation and not entirely dropped. The significance of the second shell can be seen geometrically in Fig. 1, where it is noted that the interstitial can "bond" directly with the six second-neighbor atoms giving an "effective" coordination near 10, because the second neighbors are almost as close as the first neighbors.

The energy levels of the host plus interstitial-impurity system are obtained by diagonalizing the Hamiltonian of Eq. (1). In order to study the band-gap or near-band-gap levels for a large number of impurities, it is convenient to first fix the interstitial-impurity orbital energies $\epsilon_s(I)$ and $\epsilon_p(I)$ in the block H^I to be some reference impurity energy (viz., the Si self-interstitial, with atomic orbital

TABLE I. Matrix elements (in eV) used in the calculation.

Transfer matrix element	nn_1[a]	nn_2
$W_{ss\sigma} = \langle s(\text{Si}) \vert H \vert s(I) \rangle$	-2.075	-0.812
$W_{sp\sigma} = \langle s(\text{Si}) \vert H \vert p_\sigma(I) \rangle$	2.481	0.971
$W_{pp\pi} = \langle p_\pi(\text{Si}) \vert H \vert p_\pi(I) \rangle$	-0.715	-0.280
$W_{pp\sigma} = \langle p_\sigma(\text{Si}) \vert H \vert p_\sigma(I) \rangle$	2.716	1.063

On-site matrix elements[a]

$\epsilon_s(\text{Si}) = \langle s(\text{Si}) \vert H \vert s(\text{Si}) \rangle$	-4.200	
$\epsilon_p(\text{Si}) = \langle p(\text{Si}) \vert H \vert p(\text{Si}) \rangle$	1.715	

[a]Values taken from Ref. 14.

energies in the solid[14] from Table I). Other impurities may be considered by altering the 4×4 diagonal matrix from H_{ref}^I to H_{ref}^I+V, where V (in a first, non-self-consistent approximation) is the diagonal matrix whose elements are the change in the s and p atomiclike orbital energies from those of atomic Si. The final results can be shown to be independent of the choice of the reference orbital energies if V is iterated to self-consistency, so that any reference would serve equally well. The energy levels E are determined by the determinantal equation

$$\det[1-G_{\text{ref}}(E)V]=0\ ,\tag{3}$$

where $G_{\text{ref}}(E)=(E-H_{\text{ref}})^{-1}$ is the Green's function *for the host crystal coupled to the reference Si self-interstitial,* and H_{ref} is the Hamiltonian of Eq. (1) with $H^I=H_{\text{ref}}^I$. The Green's function $G_{\text{ref}}(E)$ contains all of the information about the perfect Si host crystal and of the interactions of any interstitial impurity with its neighbors. Thus the introduction of a reference Hamiltonian for the neutral Si self-interstitial and a difference potential V has substantially reduced our computational labor since $G_{\text{ref}}(E)$ is the same for all impurities and need be computed only once.

The interstitial atom occupies a site of T_d (tetrahedral) symmetry. Symmetry arguments show that the localized levels obtained in an sp^3 basis are of A_1 (s-like) and T_2 (p-like) symmetry. These symmetry considerations factor the 4×4 determinant in Eq. (3) into a product of scalars (1×1 matrices): a singly degenerate term for the A_1 level and a triply degenerate term for the T_2 levels. The condition for a bound state simply reduces to the familiar Koster-Slater[21] condition

$$[G_{\text{ref}}(E)]_{ss}=(V_s)^{-1}\ ,$$
$$[G_{\text{ref}}(E)]_{pp}=(V_p)^{-1}\ ,\tag{4}$$

where V_s (V_p) is the orbital s (p) energy difference of the particular interstitial impurity and the reference neutral Si. The functions $[G_{\text{ref}}(E)]_{ss}$ and $[G_{\text{ref}}(E)]_{pp}$ are the on-site matrix elements of the reference Green's function

$$[G_{\text{ref}}(E)]_{ss}=\langle s(I)\,|\,(E-H_{\text{ref}})^{-1}\,|\,s(I)\rangle\ ,$$
$$[G_{\text{ref}}(E)]_{pp}=\langle p(I)\,|\,(E-H_{\text{ref}})^{-1}\,|\,p(I)\rangle\ ,\tag{5}$$

where $|s(I)\rangle$ and $|p(I)\rangle$ are the s and p atomiclike basis orbitals at the interstitial site (which need not be explicitly given).

All matrix elements of the Hamiltonian H in Eq. (1) are known explicitly, so that the necessary matrix elements of the Green's function can be found exactly (although numerically) in the model. The important diagonal terms are conveniently written (exactly) as

$$[G_{\text{ref}}(E)]_{ss}=[E-\epsilon_s(I)-\Sigma_s(E)]^{-1}\ ,$$
$$[G_{\text{ref}}(E)]_{pp}=[E-\epsilon_p(I)-\Sigma_p(E)]^{-1}\ ,\tag{6}$$

where $\Sigma_s(E)$ and $\Sigma_p(E)$ are the self-energy terms which represent the *coupling* of the interstitial atom to the surrounding host. These self-energy terms are given by[22]

$$\Sigma_s(E)=\langle s(I)\,|\,W^\dagger G_0(E)W\,|\,s(I)\rangle\ ,$$
$$\Sigma_p(E)=\langle p(I)\,|\,W^\dagger G_0(E)W\,|\,p(I)\rangle\ .\tag{7}$$

Here $G_0(E)$ is the Green's function of the *uncoupled* (i.e., $W=0$) host plus interstitial system, $G_0(E)=(E-H^0-H_{\text{ref}}^I)^{-1}$.

Hence the eigenvalue equations for the deep trap energies E are

$$E-\epsilon_s(I)-\langle s(I)\,|\,W^\dagger G_0(E)W\,|\,s(I)\rangle=V_s\tag{8a}$$

for the A_1 levels and

$$E-\epsilon_p(I)-\langle p(I)\,|\,W^\dagger G_0(E)W\,|\,p(I)\rangle=V_p\tag{8b}$$

for T_2 levels. Note that these equations require the computation of matrix elements of $G_0(E)$, which depend only on the *uncoupled* system. The impurity enters only through the energies ϵ_s and ϵ_p (and through the defect potentials V_s and V_p). The Hamiltonian of the uncoupled system block-diagonalizes to produce the perfect crystal Bloch states and the atomic energy levels of the interstitial. Note that, as the coupling potential W goes to zero, $\Sigma_i(E)$ ($i=s$ or p) goes to zero, and the Koster-Slater condition reduces to the interstitial atomic orbital energies $[E-\epsilon_i(I)]^{-1}=V_i^{-1}$, or $E=\epsilon_i(I)+V_i$, as it should. Also note that in the limit that the interstitial atom becomes an ideal vacancy ($V_s\to\infty$ and $V_p\to\infty$, Ref. 23) the spectrum of "impurity" levels for this "interstitial vacancy" is equal to the spectrum of the host, as it must be.

B. The self-consistent interstitial impurity potential

In this section, we discuss how the atomic potentials V_s and V_p of the interstitial atom are determined. First approximations to the diagonal matrix elements of the interstitial-impurity potential are the neutral free-atom orbital energies of the interstitial impurity relative to Si. However, because an interstitial impurity does not fit in with the normal bonding requirements of the surrounding host material, the charge on the interstitial atom may be quite different from that of the neutral free atom.

We include these charge-state effects in an approximate manner, using a self-consistent procedure (to be described shortly) similar to the *d*-state model of Haldane and Anderson.[16]

We begin by first constructing a phenomenological model to describe the charge-state effects on the orbital energies of a *free* atom. The Coulomb repulsion between the outer valence electrons in different spin-orbitals can be described using an Anderson[24] Hamiltonian with three electron-electron interaction parameters U_{ss}, U_{pp}, and U_{sp}. These three parameters represent the Coulomb repulsion between two *s* electrons, two *p* electrons, and an *s* and a *p* electron, respectively. Consider an atom which is successively ionized through the outer *p* and then the inner *s* shells. The atomic-orbital energies, or ionization potentials, in these different charge states are approximated by

$$E_{s\sigma}(\{n\}) = E_s^0 + \sum_{\sigma'}{}' n_{s\sigma'}U_{ss} + \sum_{j,\sigma'} n_{p_j\sigma'}U_{sp} ,$$

$$E_{p_i\sigma}(\{n\}) = E_p^0 + \sum_{j,\sigma'}{}' n_{p_j\sigma'}U_{pp} + \sum_{\sigma'} n_{s\sigma'}U_{sp} ,$$

(9)

where σ is the spin ($\uparrow$ or $\downarrow$), $i = x$, y, or z, and the prime on the summation indicates that the self-interaction ($i = j$ and/or $\sigma = \sigma'$) is excluded. Here $n_{s\sigma}$ and $n_{p_i\sigma}$ are the occupation numbers (0 or 1) of the *s* orbital and p_i orbital of spin σ, respectively. The collective set of occupation numbers is denoted by $\{n\}$. This model assumes that the atomic energies are linear functions of the electron occupancy and that quadratic effects are unimportant. That this approximation is reasonable, at least for the *p* states, can be seen in Fig. 2.

There are five unknown parameters in this phenomenological description: E_s^0, E_p^0, U_{ss}, U_{pp}, and U_{sp}. These five parameters are empirically fit so that they reproduce (i) the Hartree-Fock occupied *s* and *p* orbital energies for the neutral free atom[14,25,26] and (ii) the experimental *s* and average *p* ionization potentials.[27] The requirements (i) and (ii) yield a unique fit to the five parameters for neutral atoms which have four or more outer valence electrons.[28] However, the Coulomb repulsion between two *p* electrons, U_{pp}, is absent for neutral atoms which do not have at least two electrons in the *p* shell. Supplementary information, such as from nonionizing transitions [e.g., s^2p to sp^2 (Ref. 27)] or the excited-state calculations of Basch *et al.*,[26] is used for the lower valence atoms. The values of the Anderson *U* parameters obtained by this fitting procedure are listed in Table II.

In the solid, the orbital *s* and *p* energies of the interstitial impurity are computed using the same ap-

FIG. 2. Ionization potentials (in eV) vs number of electrons in the shell, n_p and n_s, for elements from the third row of the Periodic Table. E_s^0 is the ionization potential of the last 3*s* electron. The Coulomb parameters U_{ss} and U_{pp} [Eq. (9)] are the derivatives of the ionization potentials with respect to n_s and n_p, and can be extracted from these curves because they are nearly linear.

proximations as were made for the free-atom orbital energies in Eq. (9). The electron-electron interaction parameters *U* are assumed to be the same as those of the free atom, but since an electron is shared over many sites, the spin-orbital occupations of the interstitial $n_{s\sigma}$ and $n_{p_i\sigma}$ are no longer integers, following

TABLE II. Atomic energies E_s^{atom} and E_p^{atom} (Refs. 14, 25, and 26), bare ionization energies E_s^0 and E_p^0, as in Eq. (9), and Coulomb energies U_{ss}, U_{pp}, and U_{sp} [as in Eq. (9)].

Haldane and Anderson.[16] The spin-orbital occupation n_α (α generically denotes any one of the spin-orbitals $s\uparrow$, $s\downarrow$, $p_x\uparrow$, $p_y\uparrow$, $p_z\uparrow$, $p_x\downarrow$, $p_y\downarrow$, or $p_z\downarrow$) of the interstitial atom are obtained by integrating the local density of states $d_\alpha(E)$ for the spin-orbital α over all occupied levels,

$$n_0 = \int_{occ} d_\alpha(E)dE \ . \tag{10a}$$

The local density of states d_α is formally given by the matrix element

$$d_\alpha(E) = \langle \alpha(I) \mid \delta(E - H_{ref} - V_\alpha) \mid \alpha(I) \rangle \ . \tag{10b}$$

It is clear from Eq. (10b) that the occupation numbers n_α depend explicitly on the value of the impurity potential V_α. Conversely, the impurity potentials V_α depend on the spin-orbital interstitial-site charge occupation numbers n_α,

$$V_{s\sigma} = [E_s^0 - E_s^{atom}(Si)] + \sum_{\sigma'}{}' n_{s\sigma'}U_{ss} + \sum_{j,\sigma'} n_{p_j\sigma'}U_{sp} \ , \tag{11}$$

$$V_{p_i\sigma} = [E_p^0 - E_p^{atom}(Si)] + \sum_{j,\sigma'}{}' n_{p_j\sigma'}U_{pp} + \sum_{\sigma'} n_{s\sigma'}U_{sp} \ .$$

The prescription of Haldane and Anderson,[16] which we adopt here, is to solve Eq. (8) for the eigenvalues E, given the defect potential V_α, with the additional constraint that the resulting atomic valence configuration [Eq. (10a)] of the impurity is consistent with the input defect potential V_α.

The charge on the interstitial atom can be decomposed into two contributions; (i) a contribution n_α^{deep} from the occupied bound deep states in the band gap or from quasibound sharp resonant levels near the top of the valence-band edge, and (ii) a contribution n_α^{bands} from integrating the local density of states from below and through the valence bands to near[29] the top of the valence bands. The deep (n^{deep}) and band (n^{bands}) contributions to the occupation charge of the interstitial orbitals of A_1 and T_2 symmetry are plotted in Fig. 3 as functions of the defect potential for that orbital. (Note that $n_{A_1} = n_{s\sigma}$ for either spin σ and $n_{T_2} = n_{p_i\sigma}$.) For $V_\alpha \to -\infty$, the charge n_α^{bands} approaches unity, as expected.

The electronic occupancy $N_{l\sigma}$ of any localized levels which might be introduced into the band gap by the interstitial impurity affects the charge and potential of the impurity. (Note that $l = A_1$ or T_2 labels the levels, and that $N_{l\sigma}$, the level occupancy, is an integer and differs from n_α the fractional number of electrons in the αth orbital at the interstitial's site.) A maximum of eight one-electron levels may be formed in the gap in this model; including the spin degeneracy, there may be two of A_1 (s-like) and
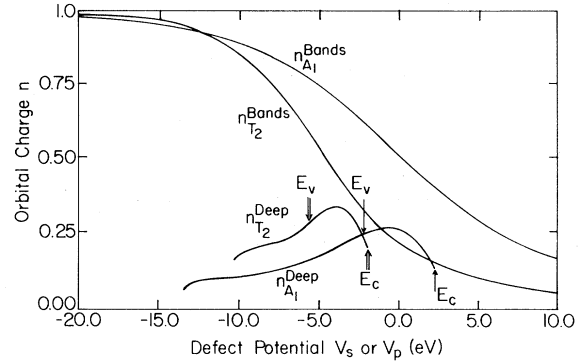
FIG. 3. Electronic charge occupancies in the solid $n_{A_1}^{bands}$, $n_{T_2}^{bands}$, $n_{A_1}^{deep}$, and $n_{T_2}^{deep}$, as defined in Eqs. (10), vs the defect potential V_s or V_p (in eV, with the Si interstitial as zero). The conduction- and valence-band edges E_c and E_v occur for defect potentials denoted by single (double) arrows for the $n_{A_1}^{deep}$ ($n_{T_2}^{deep}$). Note that for $V \to -\infty$, $n^{bands} \to 1$.

six of T_2 (p-like) symmetry. Each of these levels has a wave function $\mid \psi_{l\sigma} \rangle$ which is a linear combination of one of the interstitial-site spin-orbitals α ($\alpha = s\uparrow$, $p_x\uparrow$, $p_y\uparrow$, $p_z\uparrow$, $s\downarrow$, $p_x\downarrow$, $p_y\downarrow$, or $p_z\downarrow$) as well as several host-site spin-orbitals. The interstitial-site wave-function component $\langle \alpha(I) \mid \psi_{l\sigma} \rangle$ can be labeled by α alone, which serves as a useful index for categorizing the localized levels. Using this indexing scheme, we search for solutions of Eqs. (8) and (11) with integer occupation numbers ($N_{s\uparrow}, N_{s\downarrow}$, $N_{p_x\uparrow}, N_{p_y\uparrow}, N_{p_z\uparrow}, N_{p_x\downarrow}, N_{p_y\downarrow}, N_{p_z\downarrow}$) corresponding to each of the eight possible ground-state configurations of the interstitial impurity in each of its eight charge states (we assume A_1 levels lie lower in energy than T_2 levels):

$$(1,0,0,0,0,0,0,0), (1,1,0,0,0,0,0,0), \ldots ,$$

$$\ldots , (1,1,1,1,1,1,1,1) \ .$$

The problem of determining the impurity potential and the impurity energy levels is now completely prescribed. A specific impurity and a set of deep-level occupation numbers $\{N\}$ are selected. A trial set of V_α's are used to compute the occupation charge in each of the interstitial spin-orbitals using Eq. (10). This set of n_α's is then substituted into Eq. (11) and a new set of V_α's is generated. The procedure is repeated until self-consistency is obtained. The process is actually quite simple since most of the eight relations in Eqs. (10) and (11) are redundant. In practice there are never more than three unique defect potentials V_α and three unique interstitial spin-orbital charges n_α.

It should be emphasized that the present calcula-

tions are self-consistent and do include many-electron contributions to the interstitial's one-electron energy levels. The major approximations of the model are the treatment of self-consistency using the Haldane-Anderson procedure (which allows for the alteration of the defect potential but does not alter the neighboring host) and the neglect of lattice relaxation. Of course, both of these effects can be incorporated into the model and correspond roughly to extending the range of the defect potential. They have been omitted in the present work because we judge them unlikely to significantly alter chemical trends and because their costs in terms of lost simplicity very likely outweigh any benefits in terms of slight improvements in quantitative accuracy of the calculations.

III. QUALITATIVE PHYSICS

The *qualitative* physics of the impurity energy levels and wave functions can be understood by considering a simple molecular model. Consider a pair of molecules connected by an "interstitial" atom as shown in Fig. 4(a). The interstitial atom is assumed only to have an s state, so it only couples to the symmetric (i.e., A_1) combination of molecular orbitals of its neighbors. As shown in Fig. 4(b), there are two such combinations corresponding to linear combinations of the bonding and antibonding states of each molecule. The interstitial atom drives the bonding orbital downward to the lower energy E_1 (the interstitial atom provided an extra bond for atoms b and b') and the antibonding level to the higher-energy

level E_3. For the self-interstitial example $\epsilon_I = \epsilon_0$ shown in Fig. 4(b), the interstitial energy ϵ_I is equally pushed upward by the bonding orbital and downward by the antibonding orbital such that the level E_2, which lies in the bonding-antibonding gap, is a nonbonding orbital at the original energy ϵ_I. Altering the interstitial orbital energy ϵ_I changes the three molecular levels E_1, E_2, and E_3 as shown in Fig. 4(c). The middle branch E_2, which is the analog of the deep level, is trapped into an arctangent-shaped curve by the bonding and antibonding levels of its neighbors; this is an example of the Rayleigh interlacing theorem.[30]

A schematic plot of the wave functions for the three energy branches in this simple molecular model is shown in Fig. 4(d). Let us first focus on the wave functions of the middle "deep"-level branch E_2. The point B_2 is at an inflection point where the bonding and antibonding levels of the host are weighted equally in the construction of this deep-level wave function; here the wave function is nonbonding. As we pass through this inflection point, $A_2 \rightarrow B_2 \rightarrow C_2$, the deep-level wave-function amplitude on the interstitial atom and on its second neighbors varies slowly and smoothly. However, the deep-level wave function on the *near-neighbor* atoms changes its character dramatically; at the point A_2 below the inflection point it is negative, then vanishes at the inflection point B_2, and finally is positive (at C_2) above the inflection point. This behavior is to be contrasted with the nearly universal antibonding character of the anion-site substitutional electronegative impurity deep-level wave functions.[17,31]
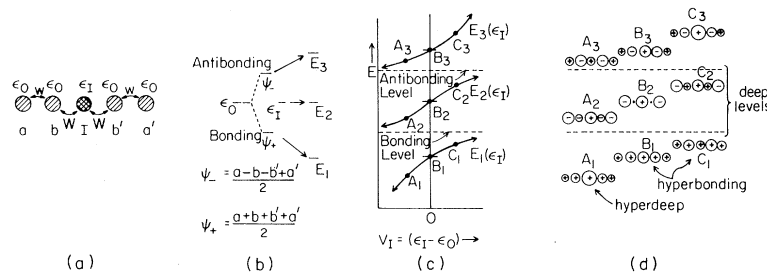
FIG. 4. Illustrating the qualitative physics of interstitial impurity levels. (a) Four atoms a, b, b', and a', with diagonal energies ϵ_0 and nearest-neighbor transfer matrix elements w, an interstitial I with diagonal energy ϵ_I and transfer matrix elements W. (b) The splitting of the host levels of a, b, b', and a' to produce the bonding state ψ_+ and the antibonding state of ψ_-. The introduction of an interstitial with $\epsilon_I = \epsilon_0$ repels the energy levels of the bonding and antibonding states, producing three levels E_1, E_2, and E_3. (c) Schematic illustration of how these levels vary as $\epsilon_I - \epsilon_0$ varies from zero. $(E_1 = B_1, E_2 = B_2, E_3 = B_3)$ to $\pm \infty$. (d) Schematic illustration of the wave functions of the levels E_1, E_2, and E_3 for conditions corresponding to different choices of ϵ_I: A, B, and C of part (c). Note that the third level E_3' retains its essential character as a conduction-band resonance, that the second level E_2 is a deep trap in this illustration, and that the second level's wave function has central-cell and second-neighbor amplitudes that are insensitive to the value of ϵ_I while the first-neighbor amplitude changes sign as ϵ_I varies. Also note that the first level changes character from a hyperdeep state that is almost completely impuritylike (for A) to a hyperbonding state for B and C, in which the interstitial's nearest neighbors develop extra bonds to the interstitial because it is nearly in resonance with them.

The wave function for the energy levels of the lower branch E_1 behaves quite differently. These levels always have bonding character but can be either impuritylike, namely *hyperdeep* in character for extremely electronegative impurities (e.g., at A_1), or hostlike (which we term *hyperbonding*) in character for electropositive impurities (e.g., at C_1). The hyperdeep level occurs when the interstitial energy level lies well below the host bonding level, and electrons flow to the highly attractive interstitial impurity. (This is similar to the hyperdeep level of substitutional impurities.[17]) As the interstitial's energy ϵ_I becomes increasingly positive ($A_1 \rightarrow B_1 \rightarrow C_1$), the charge on the interstitial spills off onto its neighbors, producing at B_1 an interstitial resonant with two neighbors (the three atoms try to share the charge nearly equally) and then a state C_1 with much of the charge on the neighbors. These last two states are largely hostlike in character and hyperbonding, because the atoms neighboring the interstitial have each developed an extra bond to the interstitial, thereby lowering the total energy of the impurity complex.

IV. RESULTS

In this section, the basic results of the self-consistent potential model are summarized. The model has been used to compute the A_1 (s-like) and T_2 (p-like) electronic levels near the band gap for each of 29 different s-p—bonded interstitial impurities in Si. A number of charge states have been considered for each impurity.

To grasp the basic general trends in the deep electronic levels, we first consider only the third-row elements Mg, Al, Si, P, S, and Cl in their neutral charge states (see Fig. 5). The levels for these impurities range from conduction-band resonances, to bound deep levels in the gap, to valence-band resonances; the most electronegative (and higher-valence) atoms producing the lowest-energy levels. The electropositive group-II element Mg produces only high-energy conduction-band resonances; its two electrons are thus captured by the long-ranged Coulomb potential, which we have omitted, into a hydrogenic shallow donor state as observed experimentally.[32] The less electropositive group-III element Al does produce a deep A_1 level just below midgap. However, its p orbital forms a T_2 conduction-band resonance whose electron is similarly lost to become a shallow donor. The Si self-interstitial produces a filled A_1 valence-band resonance level and a bound T_2 level just below the conduction-band edge. The T_2 level is so close to the conduction-band edge that it can only bind one electron; localizing a second electron increases the
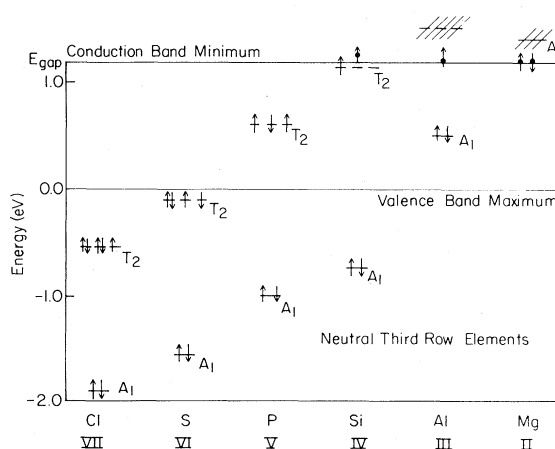
FIG. 5. Predicted chemical trends in energy levels (in eV) near the fundamental band gap for neutral third-row elements of the Periodic Table at the tetrahedral-interstitial site in Si. A_1 or s-like (T_2 or p-like) levels are denoted by single (triple) lines. Occupation by spin-up or -down electrons is denoted by arrows. (Magnetic effects and Hund's rules have been ignored in this and subsequent figures.) Deep resonances in the conduction band are hatched. Electrons that would occupy these resonances if they were genuine bound states in the gap instead spill out into the continuum and fall to the conduction-band edge (arrows with circles) where they occupy shallow donor levels as a result of the long-ranged Coulomb potential of the impurity (omitted in the present model). The zero of energy is the valence-band maximum of Si. The energies in this figure are the one-electron eigenvalues of Eq. (8), and are different for each different charge state because the mean-field Coulomb interaction, Eq. (1), is different. Some of these neutral-defect levels will be unstable to electron capture or emission (see Fig. 6). Notice that some of the predicted valence-band resonance levels are not fully occupied. Configurations associated with such levels may not be stable and the charge state of the impurity may be able to spontaneously increase by electron capture. The capture of an additional electron raises the one-electron energy level, and changes the defect's charge by one electronic charge. If the one-electron level after electron capture lies above the Fermi energy, the electron spills out of it and the original charge state is stable. If the one-electron level after electron-capture lies below the Fermi energy, either the configuration with the extra electron is the stable charge state or a configuration with more extra electrons is the stable state.

energy because of the electron-electron repulsion. The recent self-consistent pseudopotential calculations of Scheffler *et al.*[13] similarly find an A_1 valence-band resonance but only T_2 resonance levels above the conduction-band edge.

The group-I and group-II impurities which we have studied (H, Li, Be, Mg, Zn, Cd, and Hg) are all predicted to form shallow single (group-I) or double

(group-II) donors. Experimentally Li is known to be shallow[33] while H (and muonium) is believed to be deep[34–37] although its location in the lattice has not been determined experimentally. (We predict that H has a resonance ~0.3 eV above the conduction-band minimum.) One might naively expect that, since H has an atomic *s* orbital energy of -1.0 Ry which is near the Si *s* orbital energy of -1.09 Ry, the H central-cell potential would form a localized level in the valence-band similar to the Si A_1 level. However, if H were to form such a level, it would tend to

be occupied by *two* electrons, making the defect H^-, not H^0. The defect orbital energy for H^- would not be -1.0 Ry, but nearly zero; thus this occupancy effect would cause H to behave as though it were quite electropositive like Mg (but less electropositive than Li) rather than like Si.

The predictions for all the important charge states of the elements studied are shown in Figs. 6(a)–6(e). Each figure shows the energy levels for a given column of the Periodic Table. It is found that within each isoelectronic series, all of the impurities
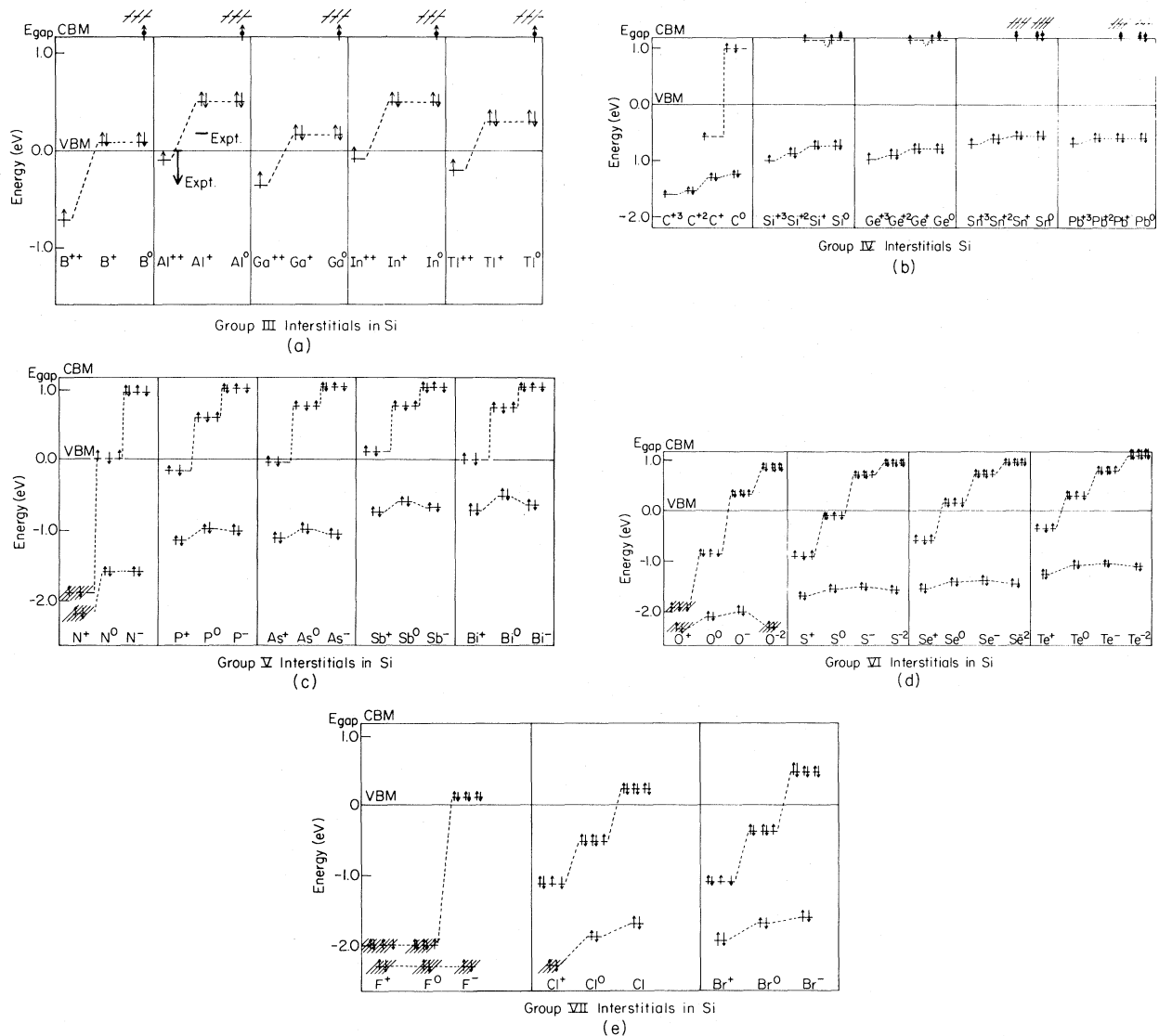
FIG. 6. Predicted chemical trends in the energy levels (in eV) for tetrahedral-site interstitial impurities of various charge states in Si. The zero of energy is the valence-band maximum. The notation is as in Fig. 5. The experimental energy levels of Al^+ (Ref. 40) and Al^{2+} [it is known only that the Al^{2+} level lies below the *p*-doped Fermi level (Refs. 1 and 39)] are given in (a). Interstitials from the following groups of the Periodic Table are given in parts (a) III, (b) IV, (c) V, (d) VI, and (e) VII. The charge states are determined as in Fig. 5. The stable charge configuration is the state with the highest one-electron level that lies below the Fermi energy.

have a very similar level structure. The second-row elements B, C, N, O, and F deviate most from the norm.

The charge-state splittings (e.g., the difference in energy levels of B^{2+} and B^+) predicted here are larger by almost a factor of 3 than those found for substitutional impurities [such as Si:Te_{Si} (Ref. 38)]. This is doubtless because of the fact that the interstitial's deep levels are more atomiclike: The charge within the central cell of the defect [which is equal to dE/dV (Ref. 31)] is approximately 3 times as large for the interstitial.

The Al interstitial provides a particularly interesting example of an interstitial impurity. This center is created in radiation damaged material. A substitutional Si atom is knocked into an interstitial position, and then migrates to the neighborhood of a substitutional Al atom. The interstitial Si and substitutional Al change places so that the interstitial impurity is now Al.[1] The material is p type (doped with substitutional Al), and the Fermi level lies slightly above the valence-band edge. Thus the Al^{2+} valence-band deep resonance level at $\sim E_v - 100$ meV [see Fig. 6(a)] represents the equilibrium state for this system. This level has an unpaired spin and is the A_1 level detected by EPR and ENDOR measurements by Watkins[1] and Brower.[39] A hyperbonding level of A_1 symmetry is predicted to lie below the valence band, but is fully occupied and is therefore not seen in EPR. By changing the Fermi level or performing a nonequilibrium experiment, the Al A_1 level can be doubly occupied (with spin ↑ and spin ↓) to produce the Al^+ center. The Coulomb repulsion between electrons drives the A_1 level out of the valence band to become a true localized band-gap deep level at $\sim E_v + 0.50$ eV as shown in Fig. 6(a). This level has been observed in deep-level transient spectroscopy experiments by Troxell et al.,[40] where they estimate the level to be at $E_v + 0.17$ eV. The third electron to be attached to the Al interstitial, forming Al^0, is predicted not to be deep and so is bound only by the long-ranged dielectrically screened Coulomb potential into a shallow donor level. This level has not been observed. Troxell et al. suggest that this is due to the interstitial atom moving out of a site of high symmetry into a site of lower symmetry such that the degeneracy of the p orbitals is removed and stronger bonds are formed.[40,41] Interstitial B^0 (Ref. 42) and C^+ (Ref. 43) are also found at lower symmetry sites, presumably for the same reason.[40]

The wave functions for the Al^{2+} center obtained from spin-resonance experiments[1,39] and from the present theory are shown in Figs. 7(a) and 7(b), respectively. The experimental wave function is reconstructed from the experimental hyperfine coupling parameters[31] assuming these parameters can be directly related to the Al and Si free-atom values of $|\psi_{atom}(0)|^2$ and $\langle r^{-3} \rangle$.[43] The Si free-atom parameters are taken from the empirically corrected Hartree-Fock values given in Ref. 44. However, we multiply the Al free-atom values of Ref. 44 by a correction factor C_{2+} (or C_+) to roughly take into account the fact that the Al^{2+} center does not involve a neutral Al atom. Hartree-Fock calculations[45] yield correction factors

$$C_{2+} = |\psi_{Al^{2+}}(0)|^2 / |\psi_{Al^0}(0)|^2 = 1.5$$

and

$$C_+ = |\psi_{Al^+}(0)|^2 / |\psi_{Al^0}(0)|^2 = 1.2 .$$

The calculation of the defect wave function is then straightforward.[46]

The experimental wave-function amplitude on the Al atom using either correction factor is shown in Fig. 7(a). Both theory and experiment show a preponderance of the wave function on the interstitial site and a much smaller amplitude on its neighbors. (Notice that we have plotted the wave-function amplitude, which exaggerates the smaller components, and not the charge density $|\psi|^2$.) The agreement of the theoretical wave function with that of experiment for the interstitial's neighbors is good, but quantitatively less impressive than for the interstitial site. The origin of this modest discrepancy is rooted in the basic nonbonding character of the interstitial deep-level wave function described qualitatively in Sec. III. There we showed that the wave function on the interstitial atom was slowly varying as a function of the deep trap energy, but that the wave function on its neighbors changes even qualitatively with small energy changes. These considerations indicate that the interstitial-site wave-function component is much easier to calculate accurately than the wave-function component of its neighbors.

Recently Elliott[47] has suggested that Ga interstitials may form a center similar to that of Al. He suggested that the Ga2 center[48] is an isolated Ga interstitial or possibly a Ga_I-Ga_{Si} pair. The luminescence (1.049 eV) is near the band-gap energy, but is split in a magnetic field into a pattern characteristic of a pair of spins $\frac{1}{2}$ instead of the usual spins $\frac{1}{2}$ and $\frac{3}{2}$ of an electron and valence-band hole. Elliott's interpretation is that the initial state is an excited Ga^+ center, where one electron is in a shallow donor level and a hole is in a tightly bound level, and the final state is the Ga^+ center in its ground state. Within the context of the present theory, this interpretation does remain plausible, since the final Ga^+ ground state does indeed lie near the valence-band edge [at $E_v + 160$ meV from Fig. 6(a)].
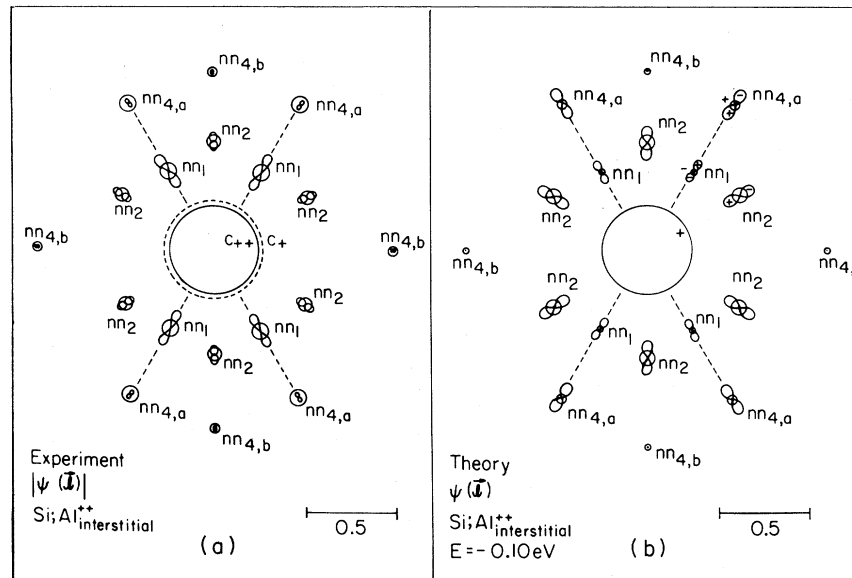
FIG. 7. (a) Experimental and (b) theoretical wave functions of the Al^{2+} interstitial at the tetrahedral site in Si. Only the magnitudes of the wave functions at the lattice sites are known experimentally. The theoretical values are obtained assuming that the interstitial level is a valence band resonance at -0.1 eV, and taking the ionic normalizations C_{2+} (solid) and C_+ (dashed) as discussed in the text. The bar in the lower-right-hand corner defines an amplitude scale of 0.5.

V. SUMMARY

We have examined the chemical trends of the energy levels of the T_d-symmetry—site interstitial *s-p*—bonded impurities in Si. The energy levels are found for 29 different impurities, each with a number of possible charge states. The theory appears to be successful in reproducing the basic chemical trends concerning which impurities form shallow, deep, or valence-band resonance levels. The major factor which determines an interstitial impurity's near-band-gap levels is the number of outer valence electrons. The group-I and -II elements studied were all found to act as shallow donors. The group-III elements already have the more complex behavior of producing valence-band resonances, deep band-gap levels, and shallow donor levels in the $2+$, $+$, and 0 charge states, respectively. Briefly summarizing the predictions for the other columns of the Periodic Table, we find that the group-IV elements generally are shallow donors, group-V and -VI impurities act as deep donors, deep acceptors, or both, and the group-VII impurities are predicted to act as deep acceptors.

The model we have used takes an atomic view of the problem. The tight-binding approximation is used for both the perfect crystal and the interstitial defect. The energy eigenvalues are determined by a

Green's-function technique where the atomiclike interstitial potential is determined self-consistently. Coulomb interaction parameters, necessary to describe charge-state effects and the self-consistent potential, are determined empirically from the free-atom orbital energies.

Comparison with known experimental data for the Al^+ center suggests that the theory is accurate to ~ 0.3 eV. (Unfortunately, a more definitive statement of the theory's accuracy is not possible, due to the lack of quantitative energy-level data for impurities known to occupy the tetrahedral interstitial site.) Although the 0.3-eV accuracy is a significant fraction of the band gap, the theory remains quite useful in understanding the global features of interstitial impurity levels and making reasonable estimates for their energies. Moreover, we doubt that currently available theoretical techniques can obtain a significantly better accuracy than this.

Finally, the theoretical wave function for the Al^{2+} center has been critically compared with the experimental wave function. Good quantitative agreement is found for the wave-function amplitude on the interstitial site; the wave-function amplitude on the interstitial's neighbors is qualitatively described, but is quantitatively less accurate than the interstitial-site wave function. We have argued on

the basis of a simple qualitative molecular model that the precise theoretical evaluation of the wave function for the interstitial's nearest neighbors is inherently a much more difficult task than for the interstitial atom itself. This is because of the basic nonbonding character of an interstitial deep-level wave function.

We hope that investigators studying interstitial defects in Si will find these guidelines useful.

[1]G. D. Watkins, *Radiation Damage in Semiconductors* (Dunod, Paris, 1967), p. 97.

[2]C. H. Henry, K. Nassau, and J. W. Shiever, Phys. Rev. B 4, 2453 (1971).

[3]G. F. Neumark, J. Appl. Phys. 51, 3383 (1980).

[4]G. G. DeLeo, G. D. Watkins, and W. B. Fowler, Phys. Rev. B 23, 1851 (1981).

[5]T. Hoshino and K. Suzuki, J. Phys. Soc. Jpn. 48, 2031 (1980).

[6]G. D. Ludwig and H. H. Woodbury, Solid State Phys. 13, 223 (1962).

[7]T. Yamaguchi, J. Phys. Soc. Jpn. 18, 368 (1963).

[8]C. Weigel, D. Peak, J. W. Corbett, G. D. Watkins, and R. P. Messmer, Phys. Rev. B 8, 2906 (1973).

[9]V. A. Singh, C. Weigel, L. M. Roth, and J. W. Corbett, Phys. Status Solidi B 100, 533 (1980).

[10]S. P. Singhal, Phys. Rev. B 4, 2497 (1971).

[11]E. Kauffer, P. Pécheur, and M. Gerl, Rev. Phys. Appl. 15, 849 (1980).

[12]C. Weigel, in *Defects and Radiation Effects in Semiconductors 1978,* edited by J. H. Albany (Institute of Physics, Bristol and London, 1979), p. 186.

[13]M. Scheffler, J. P. Vigneron, and S. T. Pantelides, Bull. Am. Phys. Soc. 27, 278 (1982).

[14]P. Vogl, H. P. Hjalmarson, and J. D. Dow, J. Phys. Chem. Solids (in press).

[15]K. C. Pandey and J. C. Phillips, Phys. Rev. Lett. 32, 1433 (1974).

[16]F. D. M. Haldane and P. W. Anderson, Phys. Rev. B 13, 2556 (1976).

[17]H. P. Hjalmarson, P. Vogl, D. J. Wolford, and J. D. Dow, Phys. Rev. Lett. 44, 810 (1980), and unpublished.

[18]P. Vogl, Phys. Rev. B (in press).

[19]W. A. Harrison, Phys. Rev. B 23, 5230 (1981).

[20]W. A. Harrison, *Electronic Structure and Properties of Solids* (Freeman, San Francisco, 1980), p. 149.

[21]G. F. Koster and J. C. Slater, Phys. Rev. 95, 1167 (1954).

[22]M. Lannoo and J. Bourgoin, *Point Defects in Semiconductors I* (Springer, Berlin, 1981), p. 84.

[23]M. Lannoo and P. Lenglart, J. Phys. Chem. Solids 30, 2409 (1969); J. Bernholc and S. T. Pantelides, Phys. Rev. B 18, 1780 (1978).

[24]P. W. Anderson, Phys. Rev. 124, 41 (1961).

[25]C. E. Fischer, At. Data 4, 301 (1972).

[26]H. Basch, A. Viste, and H. B. Gray, Theor. Chim. Acta 3, 458 (1965).

[27]C. E. Moore, *Atomic Energy Levels,* NBS Circular No. 467, Vol. I (U.S. GPO, Washington, D.C., 1949); *ibid.,* Vol. II (U.S. GPO, Washington, D.C., 1952); *ibid.,* Vol. III (U.S. GPO, Washington, D.C., 1958).

[28]As an example, we evaluate the five Anderson parameters E_s^0, E_p^0, U_{ss}, U_{pp}, and U_{sp} which enter Eq. (9) explicitly for the free sulfur atom. Neutral sulfur has four electrons in the p subshell and two electrons in the s subshell. The first four ionization energies I_1, I_2, I_3, and I_4 [10.36, 23.4, 35, and 47.29 eV, respectively (Ref. 27)] refer to p-shell electrons while the next two ionization potentials I_5 and I_6 [72.5 and 88.03 eV, respectively (Ref. 27)] refer to s-shell electrons. The ioniziation energy I_6 is that of a bare s electron, so the parameter E_s^0 is -88.03 eV. The difference $I_6 - I_5$ is 15.53 eV and is the interaction between two s electrons U_{ss}. The average difference between p-shell ionization energies, $(I_2 - I_1)/3 + (I_3 - I_2)/3 + (I_4 - I_3)/3$, is 12.31 eV and represents the average repulsive interaction U_{pp} between two p electrons. The last two parameters U_{sp} and E_p^0 are obtained by fitting to the neutral-atom Hartree-Fock energies (E_s^{atom} and E_p^{atom} in Table II), that is,

$$U_{sp} = [E_s^{\text{atom}} - E_s^0 - (n_s - 1)U_{ss}]/n_p$$

$$= 12.15 \text{ eV}$$

and

$$E_p^0 = E_p^{\text{atom}} - (n_p - 1)U_{pp} - n_s U_{sp}$$

$$= 73.12 \text{ eV} ,$$

where for the neutral atom n_s and n_p are 2 and 4, respectively.

[29]The contribution of the bands to the charge on the interstitial atom is obtained by integrating the energy E in Eq. (10a) from $-\infty$ to -1.60 eV for A_1 states and from $-\infty$ to -1.25 eV for T_2 states.

[30]See, for example, A. A. Maradudin, E. W. Montroll, and G. H. Weiss, Solid State Phys. Suppl. 3, 132 (1963).

[31]S. Y. Ren, W. M. Hu, O, F. Sankey, and J. D. Dow, Phys. Rev. B 26, 3750 (1982).

[32]L. T. Ho and A. K. Ramdas, Phys. Rev. B 5, 462 (1972); Phys. Lett. 32A, 23 (1970).

[33]C. Jagannath, Z. W. Grabowski, and A. K. Ramdas,

Phys. Rev. B $\underline{23}$, 2082 (1981); C. Jagannath and A. K. Ramdas, *ibid.* $\underline{23}$, 4426 (1981).

[34]J. H. Brewer, K. M. Crowe, F. N. Gygax, R. F. Johnson, and B. D. Patterson, Phys. Rev. Lett. $\underline{31}$, 143 (1973).

[35]J. Shy-Yih Wang and C. Kittel, Phys. Rev. B $\underline{7}$, 713 (1973).

[36]M. Altarelli and W. Y. Hsu, Phys. Rev. Lett. $\underline{43}$, 1346 (1979).

[37]L. Resca and R. Resta, Solid State Commun. $\underline{29}$, 275 (1979).

[38]H. G. Grimmeiss, E. Janzén, H. Ennen, O. Schirmer, J. Schneider, R. Wörner, C. Holm, E. Sirtl, and P. Wagner, Phys. Rev. B $\underline{24}$, 4571 (1981).

[39]K. L. Brower, Phys. Rev. B $\underline{1}$, 1908 (1970).

[40]J. R. Troxell, A. P. Chatterjee, G. D. Watkins, and L. C. Kimerling, Phys. Rev. B $\underline{19}$, 5336 (1979).

[41]G. D. Watkins, in *Radiation Damage and Defects in Semiconductors*, edited by J. E. Whitehouse (Institute of Physics, Bristol and London, 1973), p. 228.

[42]G. D. Watkins, Phys. Rev. B $\underline{12}$, 5824 (1975).

[43]G. D. Watkins and K. L. Brower, Phys. Rev. Lett. $\underline{36}$, 1329 (1976).

[44]G. D. Watkins and J. W. Corbett, Phys. Rev. $\underline{134}$, A1359 (1964).

[45]J. Boisvert, J. Blaisdell, and A. B. Kunz (private communication).

[46]The tight-binding model gives directly the projection $c_i(\vec{R})$ of the deep-level wave function $\psi(r)$ on the localized basis orbital $\phi_i(\vec{r}-\vec{R})$ of the atom at site $\vec{R}$,

$$c_i(\vec{R}) = \langle \psi(\vec{r}) \mid \phi_i(\vec{r}-\vec{R}) \rangle^* \,,$$

where $i = s$, p_x, p_y, p_z, or s^*. Spin resonance experiments in Si are generally interpreted within the approximation that the localized basis orbitals are the $3s$ and $3p$ orbitals of a free Si atom. In this approximation the hyperfine parameters of the atom at site $\vec{R}$ depend on

$$\mid c_s(\vec{R}) \mid^2 \mid \phi_s^{\text{atom}}(\vec{R}) \mid^2$$

and $\mid c_p(\vec{R}) \mid^2 \langle r^{-3} \rangle$, where we have

$$\langle r^{-3} \rangle = \langle \phi_p^{\text{atom}} \mid r^{-3} \mid \phi_p^{\text{atom}} \rangle \,.$$

Since the quantities $\mid \phi_s^{\text{atom}}(\vec{R}) \mid^2$ and $\langle r^{-3} \rangle$ for the free atom are known (see Refs. 44 and 45), approximate experimental measurements of $\mid c_s(\vec{R}) \mid^2$ and $\mid c_p(\vec{R}) \mid^2$ are obtained, which are then compared with the present theory.

[47]K. R. Elliott, Phys. Rev. B $\underline{25}$, 1460 (1982).

[48]J. R. Noonan, C. G. Kirkpatrick, and B. G. Streetman, Solid State Commun. $\underline{15}$, 1055 (1974).